

## 2 RESEARCH

### 2.1 Origin and Composition of Cosmic Rays

Marco Arosio

Cosmic Rays are highly energetic particles, generally protons and electrons, which travel in the interstellar medium at velocities near the speed of light. Their interaction with the molecules constituting the Earth's atmosphere produces showers of energetic secondary particles that can be detected at ground level.

Cosmic rays have a wide range of energies. From the lower limit, which is conventionally taken as  $mc^2$  (e.g. approximately 1GeV for a proton), particles have been detected with energies exceeding  $10^{20}$  eV. As an example, the highest energy that can be produced in an accelerator on Earth is of the order of  $10^{12}$  eV. This can be done at Fermilab's Tevatron, the world's largest particle accelerator. Ordinary stars cannot account for the production of most of the energies measured. The determination of the origin is complicated by the fact that, unlike photons, the path of charged particles, such as protons and electrons, can be deflected by magnetic fields present in our galaxy. It follows that the trajectories of cosmic rays detected on the Earth's surface do not point back to their sources. The determination of the origin has to rely on indirect methods. While the sources for energies up to  $10^{15}$  eV seem to have been located, studies are currently focusing on the type of processes able to generate the rarer highest energies.

#### Primary and Secondary Cosmic Rays

Cosmic rays are classified into two categories. Primary cosmic rays consist of all the particles arriving to Earth from space. The primary rays do not usually make it to the surface of the Earth, and constitute only a small fraction of what is detected at ground level. Secondary cosmic rays instead are what are detected at ground level. In other words, they comprise all the particles being created in the interaction of the primary ray with the constituent atoms of the upper atmosphere. When a high energy proton, as part of a cosmic ray, hits the nucleus of an atom of the air many hadrons are in fact produced, of which a large amount are pions (Figure 1, below).

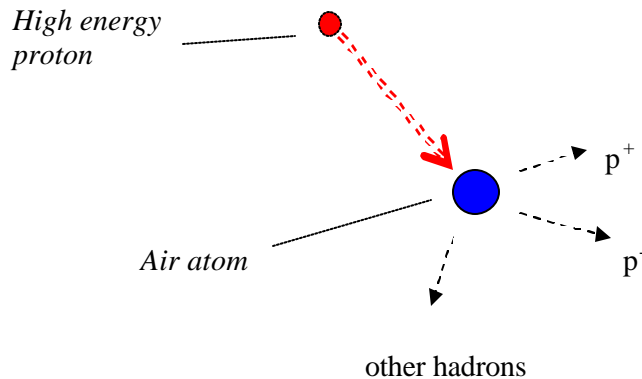


Figure 1: Diagram of particle interactions in air

Many of the particles created in the collisions are short-lived and do not survive to reach sea level, but positive and negative pions created in the process decay into muons that can be detected at ground level due to relativistic effects. Those muons that are produced with a high enough energy have their lifetime with respect to the earth's frame relativistically dilated and it is possible for them to reach the ground before decaying.

There exist two types of muon: positive and negative. If a negative muon ends its path in some material, then it can be captured into an orbit around the nucleus of an atom and interact. Positive muons instead are repelled by the nucleus and decay in isolation.

The decay of a positive muon has the following reaction equation (1):



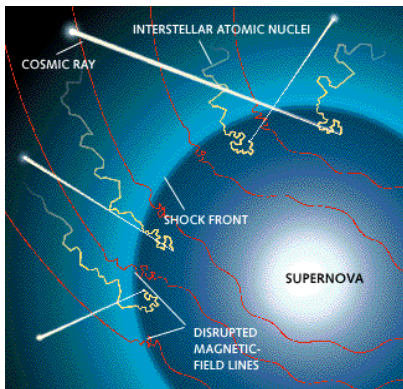
If a negative muon decays before it interacts with the nucleus, the process has the reaction shown by equation (2):



By inspection, it can be seen that the main product of a muon decay is either an electron or a positron. Because they are much more massive than electrons, muons readily pass through the electric fields inside matter with very little deflection, so do not radiate and slow down as electrons do. However they can cause ionisation and this makes them readily detectable in matter, for example with a Geiger counter.

## Supernovae

Recent studies have located the source of most of the Cosmic Rays that reach our planet to be outside the Solar System but within our galaxy. The explosive deaths of massive stars, supernovas, are thought to be responsible for the production of ordinary Cosmic Rays with energies up to  $10^{15}$  eV. Studies of the spectra of Supernova remnants found that the majority of the X-Ray emission comes from hot gas surrounding the remnant. The gas gets heated by the supernova shock wave as it goes through interstellar space. The hot gas then emits X-rays via thermal emission. In addition, some of the interstellar gas can get trapped in the supernova's shock wave



and start to bounce back and forth across the shock region in a process known as Fermi acceleration. The more times the electrons, protons and ions from the gas bounce back and forth, the more energy they gain. These particles then eventually escape the wave front and become cosmic rays. The occurrence of this type of process is confirmed by the observation of synchrotron radiation emission lines in the remnant's spectrum. This is due to the interaction of cosmic ray electrons with the high and extensive magnetic fields surrounding the remnant.

**Figure 2: cosmic ray production in supernova shock wave**

(<http://www.maclester.edu/astronomy/people/mattc/CROrigin.htm>)

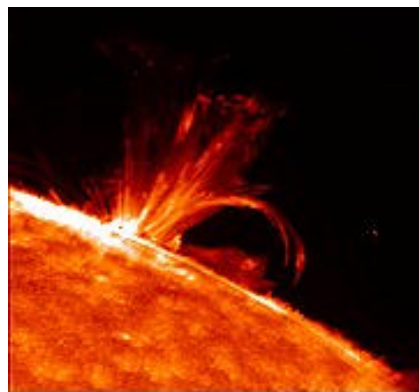
A good example of a source of cosmic rays is the Crab nebula in the Taurus constellation (see fig.3, below). The nebula is in fact the remnant of a supernova explosion that was observed in 1054 by Chinese and Arab astronomers. The explosion of the star produced a large expanding shell of ionised gases. Energetic electrons moving at high speeds through the magnetic fields of the remnant emit strong observed synchrotron radiation. The nebula is also a strong emitter of X rays. At its centre is a pulsar, or neutron star, spinning about 30 times per second.



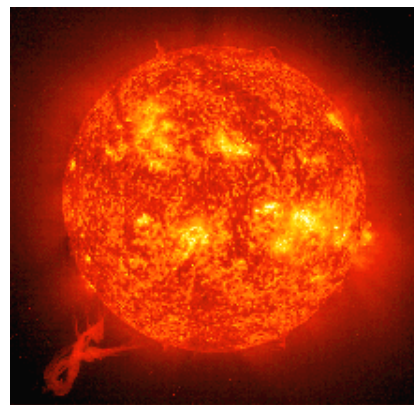
**Figure 3: The Crab nebula.**  
(<http://csep10.phys.utk.edu/guidry/violence/gifs/n1952noao-crab.jpg>)

### Solar Cosmic Rays

The Sun is a known source of cosmic rays. The Solar Cosmic Rays, whose main constituents are single protons and electrons, reach the Earth through the solar wind which originates in the Sun's corona. Energetic particles are produced in high energy explosions, or solar flares, occurring in the Sun's atmosphere (Figure 4, below).



A solar flare NASA



NASA

**Figure 4: Solar flares in the Sun's atmosphere**  
([http://www.riverdeep.net/current/2001/06/061801t\\_solar.jhtml](http://www.riverdeep.net/current/2001/06/061801t_solar.jhtml))

A few particles detected on Earth can be associated with these violent events occurring in the Sun's atmosphere, but the bulk of cosmic rays show an anticorrelation with solar activity, proving the existence of sources of a different nature, e.g. supernovas. The solar cosmic rays have in fact very low energies and except for a minute fraction they are all deflected by the Earth's magnetic field and absorbed in the atmosphere.

The absorption process, which ionizes gases in the upper atmosphere, accounts for the phenomenon of Aurorae (Figure 5, below). The Sun also plays another role in the physics of Cosmic Rays: rays entering the Solar System lose some of their energy due to the action the Sun's magnetic field, whose strength is transmitted to the outer regions of the Solar System by the solar wind.



**Figure 5: Aurora Borealis**

(<http://www.geo.mtu.edu/weather/aurora/images/aurora/jan.curtis/index.html>)

### Ultra-high Energy Cosmic Rays

Ultra-high Energy Cosmic Rays are so called because of their enormous energies, sometimes exceeding  $10^{20}$  eV. There is still no clear understanding of the type of processes able to produce such energies. As calculations showed that they could not be generated by supernovas, first research identified high energy objects such as quasars and Gamma ray bursts located billions of light years away from Earth as potential sources of ultra-high energy cosmic rays. Later studies proved the impossibility of such high energy rays coming from such far distances. Cosmic ray protons with energies above  $10^{19}$  eV are likely to collide with the photons of Cosmic Microwave Background Radiation and therefore lose some of their energy. It has been calculated that no cosmic ray can travel more than 100 million light years before falling below the  $10^{19}$  eV threshold energy, which is about the size of the local supercluster of galaxies. Analysing data from high energy cosmic ray detectors, researchers have recently traced the trajectories of several of the particles to four relatively close galaxies known to surround dead or dormant quasars and which are suspected to contain supermassive black holes.

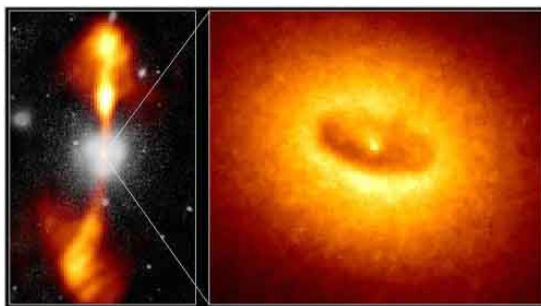


**Figure 6: Radio telescope image of active galaxy NGC-4261(left) and close up image from the Hubble Space Telescope(right).**

(<http://ast.leeds.ac.uk/haverah/high.shtml>)

Figure 6, above, shows a potential source of ultra-high energy cosmic rays. The ring at the core of the galaxy is thought to orbit a giant black hole. The spinning hole would drag magnetic field lines through the gas around it and this in turn would induce a super-strong electric field that could accelerate particles to the desired energies. This is possible if the galaxy does not display any quasar-like activity, since interactions with the ambient quasar radiation can drain the particles of most of their energy. In practice, the detection of ultra-high energy cosmic rays is a very rare

phenomenon. In fact only one high energy particle arrives per square kilometre per decade.

## 2.2 Cosmic Ray Flux at the Earth's Surface

Manuel Kurdian

Cosmic rays originating from the Sun, the galaxy and beyond are subject to modulation caused by solar activity, which has a twenty two-year cycle. Particles of solar origin are few and are associated with the violent processes occurring on the surface of the Sun called solar flares and prominences, which are more frequent at the solar maximum and are subject to rapid variations. The Sun also ejects a constant stream of magnetised plasma from its upper atmosphere, which constitutes the solar wind. This magnetized plasma becomes turbulent on expansion at times of high solar activity as seen in figure 7, which affects the propagation of, and therefore partially excludes, the extra-solar cosmic ray flux from the inner solar system. This anti-correlation of the intensity is significant for cosmic rays of an energy spectrum below 10GeV.

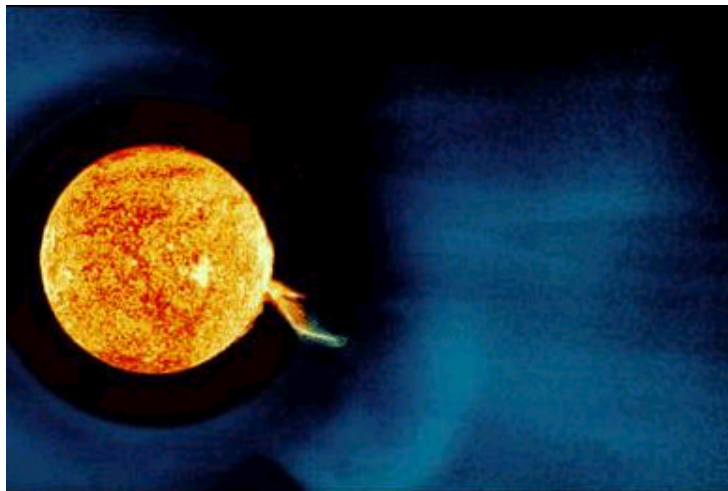


**Figure 7: A coronal transient (light blue) expanding outwards from the Sun, propelled by a prominence.** The prominence is shown in the ultraviolet image of the Sun which has been superimposed over the dark circle of the coronagraph used to image the corona.  
*NASA / JPL – Skylab.*

Cosmic rays of solar and extra-solar origin are both hindered by the geomagnetic field. The particles in the solar wind travel at supersonic speeds of approximately 400km/s, which are deflected thus forming a cavity in the solar wind called the magnetosphere on reaching the geomagnetic field. At the first contact of the particles with the magnetic field they suddenly slow down to subsonic speeds at the boundary called a shock wave (see figure 8, overleaf). Closer to the Earth there is another boundary called the magnetopause where the outward magnetic pressure of the Earth counterbalances the pressure of the solar wind. It is along this boundary that most of the particles are deflected as water from a tap does over a solid sphere in its path.

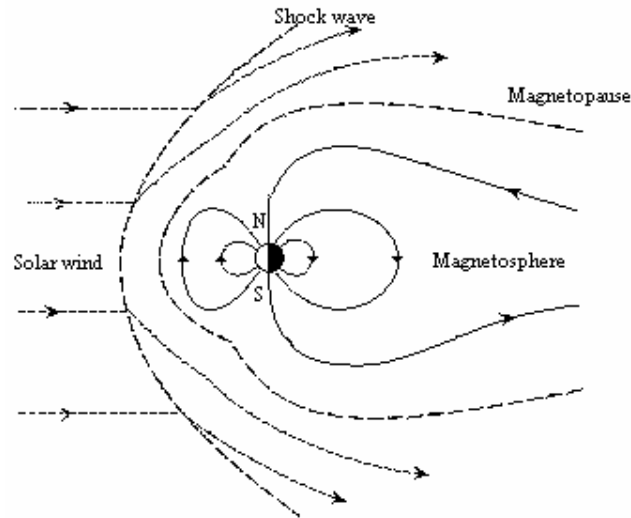


**Figure 8. A sketch showing the structure of the cavity which the Earth's magnetic field produces in the solar wind.**

*Taken and altered from [http://www.agu.org/sci\\_soc/cowley.html](http://www.agu.org/sci_soc/cowley.html).*

The moving charged particles interact with the geomagnetic field in such a way as to generate huge electric currents of high speed particles along the magnetic field lines. These are directed towards the magnetic poles of the Earth in the same manner as a dynamo generates electrical current by the movement of a conductor through a magnetic field. This results in increased interactions of particles with the atmosphere near the Earth's north and south poles thus producing such phenomena as the northern (aurora borealis) and southern (aurora australis) lights (see figure 9, below). The effects of the geomagnetic field are significant for particles of energy less than 1GeV.

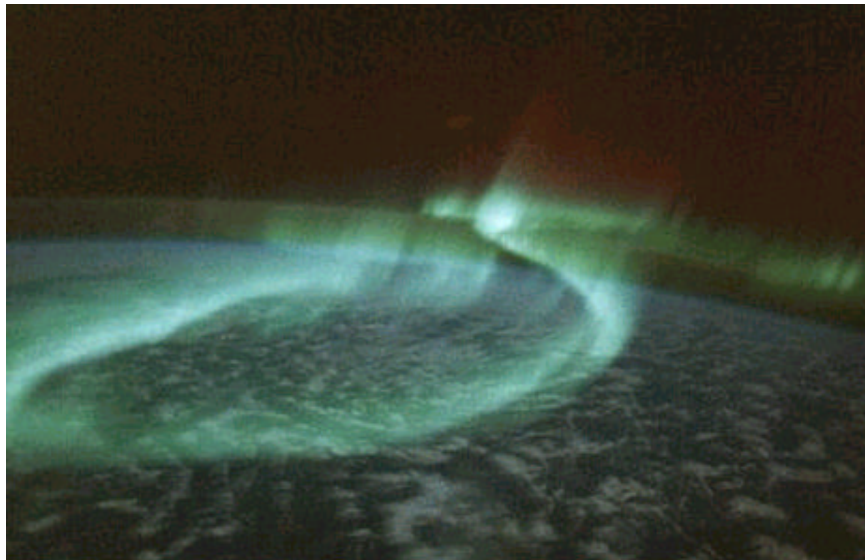


**Figure 9. Aurora Australis, photographed from Discovery's flight deck by one of its crew members (NASA)**

We can therefore see that the intensity of cosmic rays depends both on location and time on the surface of the Earth.

Muons are the most numerous particles which are detected at sea level. They are produced at roughly an altitude of 15 km and lose approximately 2GeV of energy due to ionisation before they reach the ground. The primary cosmic rays which impact the atmosphere to form these muons must have a minimum energy of 450MeV per nucleon in order to generate particles detectable at sea level.

Muons have a decay length, which is energy dependent. As the angle of detection from the zenith ( $\theta$ ) increases (see figure 10, below), muons would have to travel longer distances for a given angle to reach the surface where the detector is. Thus low energy muons decay before they reach the surface, giving an angular distribution approximately proportional to  $\cos^2 \theta$  for muons with an average energy of 3GeV. This steepens for lower energy and flattens for higher energies.

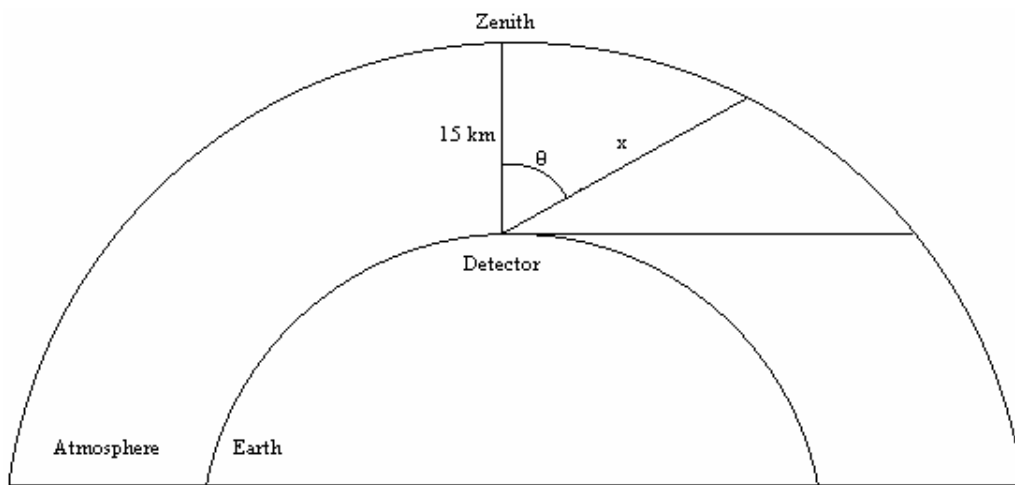


**Figure 10.** Demonstration of how the distance to the detector at the surface changes with angle  $\theta$  from the zenith.

Pions (from primary cosmic rays) also decay before they interact with the atmosphere to form Muons, therefore the average energy of Muons increases with angle  $\theta$  from the zenith.

## 2.3 The History of Cosmic Ray Physics

Caroline Robson

The history of cosmic ray physics began around 1900, when it was discovered that an electroscope (an instrument used to detect ionising radiation, see fig.11, below) still discharged when it was kept well away from sources of natural radiation. These events were observed to occur even when the electroscope was surrounded by 10cm of lead. Many experiments were devised to try and discover the source of this highly penetrating radiation.

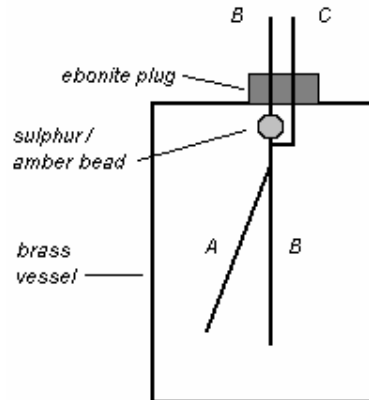


**Fig.11: The gold-leaf electroscope.** A strip of gold leaf (A) is attached to a flat rod (B) at one end and these are insulated inside a brass vessel by a small bead made of amber or sulphur, both of which are almost perfect insulators in dry conditions. The rod and the gold leaf are charged by another rod (C) which passes through the side of the vessel via an ebonite plug and is connected to a 200-300V battery. Once the leaf and rod B are charged the charging rod C is removed and connected to earth, as is the portion of rod B that lies above the bead. The presence of conducting ions, caused by ionising radiation, results in leakage currents in the gold leaf, causing it to discharge and move towards the rod. The rate at which this happens is directly related to the amount of ionisation.

An experiment carried out in 1910 by Wulf, a respected manufacturer of electroscopes, showed that the ionisation measured at the top of the Eiffel Tower, at a height of 330m, was  $3.5 \times 10^6$  ion pairs  $\text{m}^{-3}$ , which was just over half that measured at the bottom ( $6.0 \times 10^6$  ion pairs  $\text{m}^{-3}$ ). At the time  $\gamma$ -rays were thought to be the most penetrating type of ionising radiation and using their known air absorption coefficient



it was calculated that if they had originated from natural sources on the Earth's surface the ionisation rate would have halved by a height of 80m. At the top of the Eiffel Tower it would have been almost undetectable. In 1912 and 1913 the Austrian physicist Victor Hess and the German Werner Kolhorster made hot air balloon ascents in order to measure the change in ionisation with increasing altitude. Hess flew to altitudes of around 5km and was the first to discover that the source of the ionising radiation lay outside of the Earth's atmosphere (see fig.12). He was awarded the Nobel Prize in 1936 for his work in this field.

**Fig.12: Hess returning from a successful balloon flight**

(<http://ast.leeds.ac.uk/haverah/cosrays.shtml>)

Kolhorster made ascents to 9km and found that the particle flux, although decreasing slightly at first, increased rapidly from a height of 1500m up to a 10-fold increase with respect to the value at sea level. Further flights were made by Robert Millikan and Ira Bowen in the US, convincing themselves and the scientific community that the radiation was coming from outside the atmosphere. They were named 'cosmic rays' by Millikan in 1925.

In 1929, the invention of the Geiger-Müller detector allowed single cosmic rays to be detected and their arrival times to be determined to a high level of accuracy (see fig.13, below). Kolhorster and Walther Bothe commenced an experiment to discover whether the radiation consisted of  $\gamma$ -rays or, as suspected, charged particles. They pioneered the technique of using coincidence detection to eliminate background. Using two counters, one on top of the other, an event was only recorded if detected by both counters at the same time. This set up is known as a GM telescope, as it can determine the incident direction of a particle depending on the arrangement of the detectors. It was found that even when a strong absorber was placed between the two detectors, simultaneous discharges were found to occur often. If they had been  $\gamma$ -rays, each one would have had to produce two secondary electrons which travel in the same direction and are subsequently detected at the same time by both detectors. The low probability of this happening, coupled with the high count rate observed, implied that the cosmic rays being detected were highly-penetrating charged particles, detected directly by the GM counters. The particles were estimated to have energies of  $10^9 - 10^{10}$  eV.

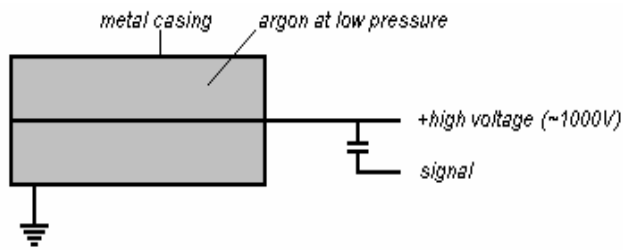


**Fig.13: A Geiger-Müller detector.** The detector consists of a metal cylinder containing argon at low pressure. A high voltage is maintained between the wall of the cylinder and a thin wire fixed along its axis. Ionising particles entering the tube cause electron cascades which create detectable pulses of electric current.

Around the same time, an apparatus called a cloud chamber was developed by Charles Wilson at Cambridge and became a standard detection method for many years. Wilson discovered that when water was sprayed into a chamber of gas at very low pressure, clouds would form if there were enough dust particles to act as nucleation sites for the water to condense on. He found that even when the chamber had been completely cleaned of dust particles, clouds were still able to form and this effect was increased by directing an X-ray beam into the chamber. It was concluded that ions were responsible for the formation of the clouds and that ionising radiation entering the chamber could leave tracks of which photographs could be taken for analysis. An applied magnetic field could be used to curve the paths of the particles and from the photographs the mass and charge of each incident particle could be determined.

The cloud chamber was instrumental in the discovery of the positron, the electron's antiparticle, by Carl Anderson in 1936. However other cloud tracks were often seen which curved much less than the electron and positron tracks and did not demonstrate any interactions between the particle and the gas inside the chamber. These new particles, or 'mesotrons' as they were called at the time, were estimated to have a mass 200 times that of the electron but the same unit of charge. These are now called muons and are known to be secondary particles of cosmic ray interactions in the atmosphere. Anderson shared the 1936 Nobel Prize with Victor Hess.

In 1935, experiments had begun using photographic emulsions to track the trajectories of particles. This technique was based upon Rutherford's early experiments with

$\alpha$ -particles using photographic plates. In November of that year, plates were carried into the stratosphere aboard Explorer II by Capts. Albert Stevens and Orvil Anderson of the US Army. When the plates were developed, the tracks of primary cosmic rays were observed. In 1947, using more sensitive emulsions developed by Cecil Powell of the University of Bristol and the photographic companies Kodak and Ilford, tracks of another particle, the pion, were observed as well as muons, now known to be their decay products. The existence of the pion had been predicted by Hideki Yukawa in 1936. He had proposed that the strong force that held together protons and neutrons in atomic nuclei was due to the exchange of particles with a mass of around 250 times that of the electron. Charged pions are the product of cosmic ray interactions with the gases in the upper atmosphere.

Until the 1950s, cosmic rays were used extensively in particle physics experiments. By 1953, the technology used to build particle accelerators had developed enough to allow beams of particles with sufficient energy for these experiments to be produced in the laboratory. However, the most energetic particles discovered in cosmic ray showers have energies of  $10^8$  times that of those that can be produced in an accelerator.

As most of the cosmic ray particles detected at sea level are secondary products of interactions that took place at the top of the atmosphere, studies of the origins of cosmic rays could only be carried out from the 1960s onwards, when it has been possible to send detectors into space aboard satellites.

## 2.4 Modern Detection Techniques

Modern detectors have come a long way from the instruments used in the early detection of cosmic rays. Several methods were researched in order for the design of a portable detector to be developed.

### 2.4.1 Spark Chambers

Rebecca Wong

A spark chamber is a radiation detector used in the investigation of subatomic particles in high-energy particle physics. Particles pass through a stack of metal plates or wire grids that are maintained with high voltage between alternate layers. A high-pressure gas fills the gaps between the plates and is ionized along the path of the traversing charged particle. As a result, sparks jump between adjacent, oppositely charged plates and the trail of sparks left by the particle is seen as a series of dashes.

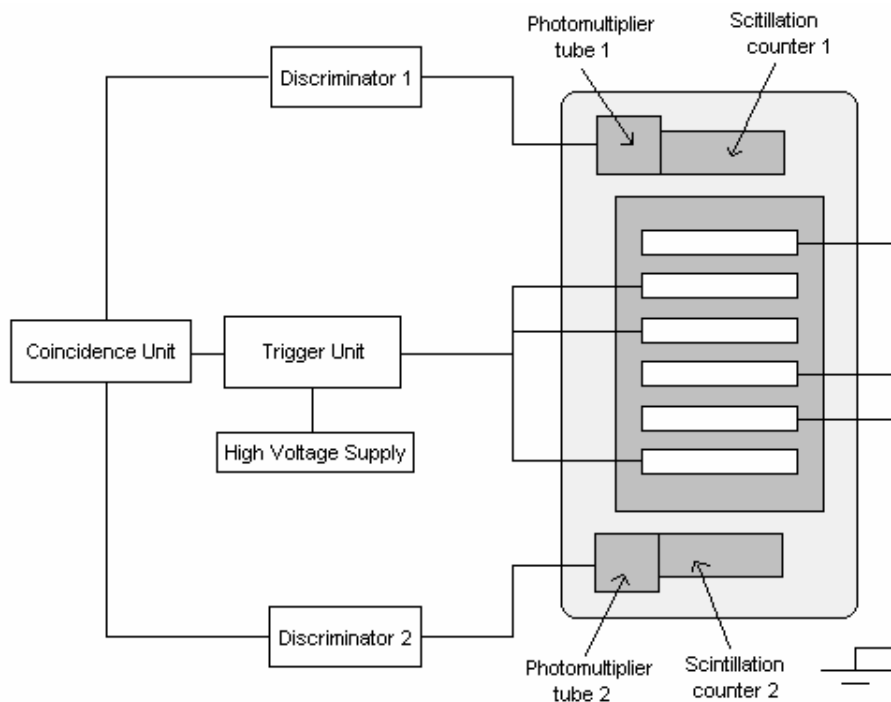


**Fig 14: Circuit Diagram of a spark chamber.**

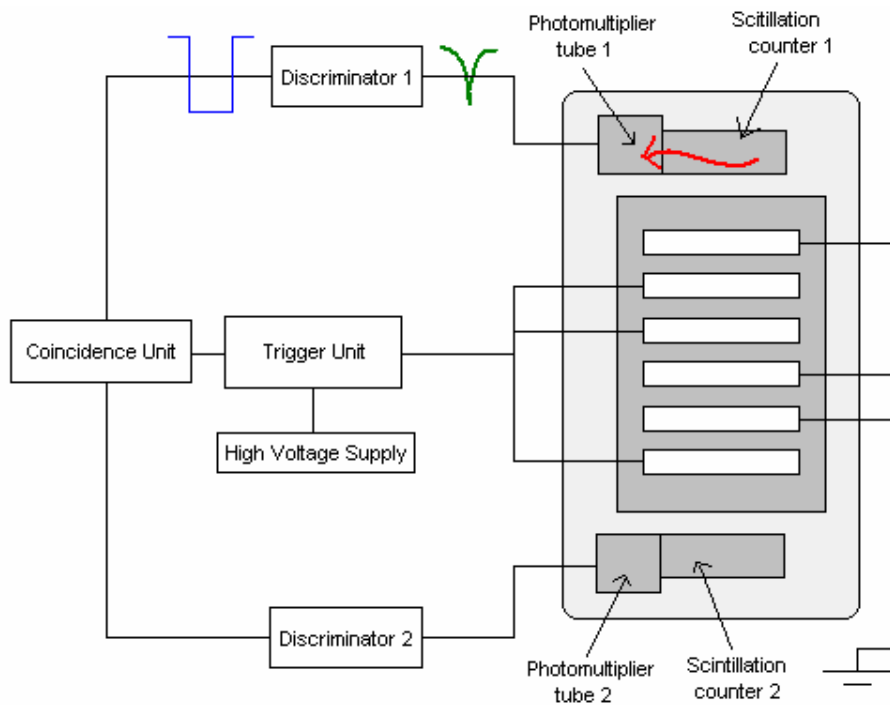
(The components in the light grey box are the 'detector' components of the spark chamber)

Fig 14 above shows a typical circuit of a spark chamber. The spark chamber consists of stacks of modules, each module consisting of a perspex frame. On the top and bottom of these perspex frames are glued aluminium plates. For each module, one aluminium plate is connected to ground while the other is connected to the High Voltage (HV) circuit.

The active volume of each module within the perspex frame and between the aluminium plates is filled with a noble gas mixture (70% Neon, 30% Helium). The gas flows in series from one module to the next, through all of the modules.

At the top and bottom of the spark chamber, covering the active area of the modules, are located two scintillation counters. When the scintillation counters are traversed by a charged particle, the ionisation produced may recombine, emitting visible light. The photons are detected by a photomultiplier tube. Since both the scintillation counter and phototube have a fast response time, the resulting electrical signals indicate in a very short time the passage of a charged particle.

### How does a spark chamber work?



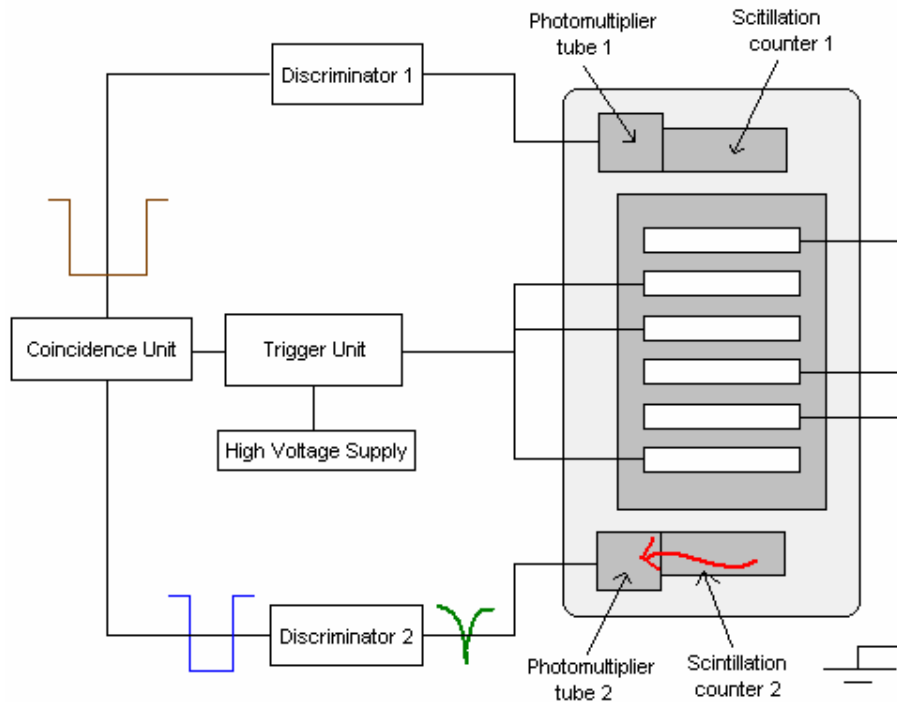
**Fig 15: First stage for the spark chamber to detect cosmic rays**

Fig 15 above shows the first stage of the detection process for the spark chamber. When a cosmic ray enters the spark chamber through the scintillator 1, it causes a photon (shown in blue on fig.15, above) to be emitted, and is detected by the phototube 1. The light pulse is then converted into an analogue electrical signal (shown in green). This signal is then passed into discriminator 1 where the analogue signal is converted into a digital one (shown in blue). The cosmic ray has now passed through the stacks of modules, leaving the noble gas mixture ionised.

On exiting the chamber the cosmic ray passes through the second scintillation counter (shown on fig 16, next page) which, like the first counter, emits a photon which is detected by phototube 2, then converted into an analogue signal. This signal is then passed through discriminator 2 where the analogue signal is converted into a digital one before passing into the coincidence unit.

The coincidence unit gives an output (shown in brown on fig. 16) when it receives the digital signals from the two discriminators within a certain time interval. These

simultaneous signals indicate the passage of a charged particle through the spark chamber.



**Fig 16: Second stage for the spark chamber to detect cosmic rays**

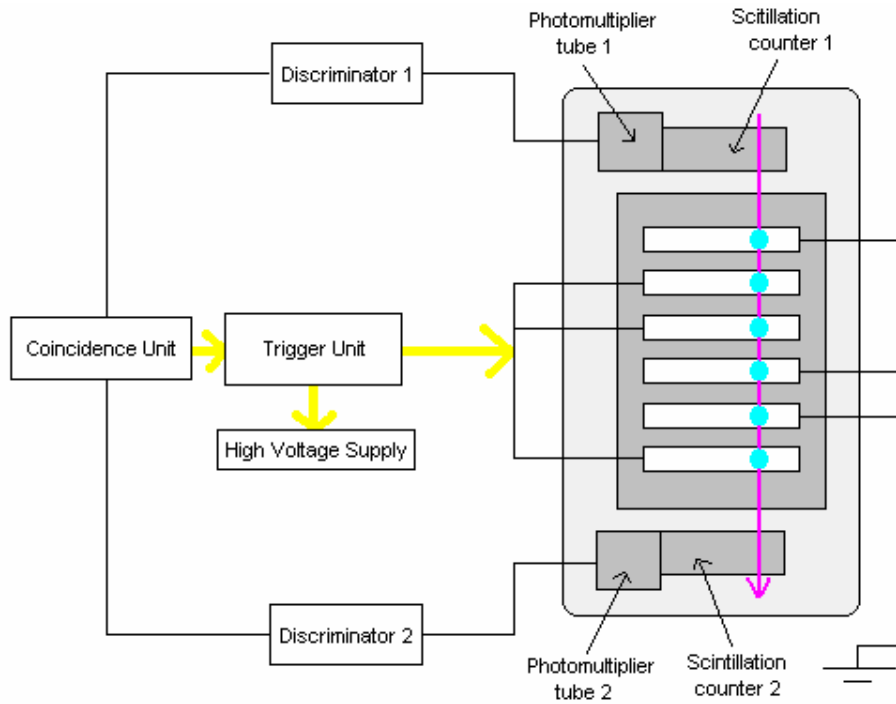


**Fig 17: Final stage for the spark chamber to detect cosmic rays**

If the coincidence unit receives a signal from the top and bottom scintillator together, then it will pass a signal to the triggering unit (as shown in fig.17, previous page). The triggering unit is a capacitor charged up to a high voltage. On receiving the signal from the coincidence unit this capacitor will be caused to discharge and approximately 80% of the high voltage will be applied to one of the two plates of each module.

Thus a potential difference exists across each module. In this unstable situation, the modules cannot stay like it for any length of time. The plates must discharge.

This discharge will occur along the easiest path possible. The easiest path is through the ionised track left behind in the noble gas mixture by the passage of a cosmic ray. The plates will discharge down the ionised track of the cosmic ray, and hence the characteristic spark and the 'crack' sound from the discharge are observed

The light blue circles shown on fig.17, previous page, are the sparks along the track of the cosmic ray which the spark chamber has detected.

### Why does the Spark Chamber Spark?

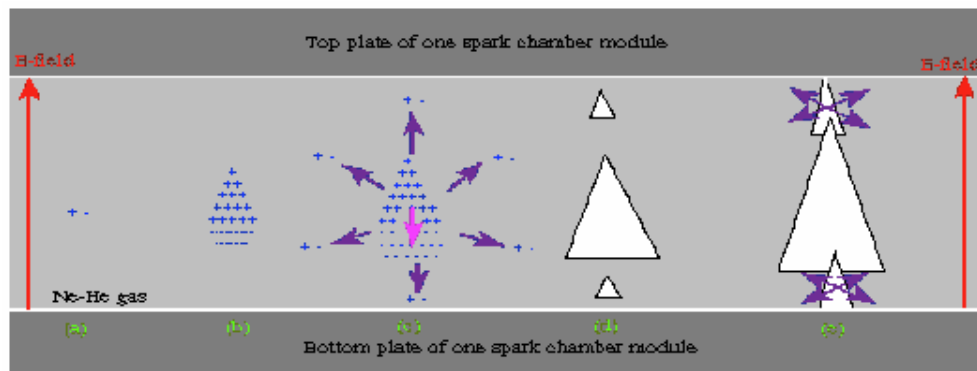


**Fig 18: Stages of spark formation within 1 module of the spark chamber**  
(From Birmingham University, School of Physics and Astronomy website)

A large potential difference across the closely spaced parallel plates of each module has associated with it an electric field in the vicinity of the plates (as shown in fig.18, above). An electron present in the active region of each module, which is created from the ionisation of the gas mixture as a charged particle traverses the chamber, is accelerated towards the anode plate (a).

As the electron travels, its energy increases and becomes sufficient to cause ionisation when it collides with a gas molecule in its path. An additional electron is liberated which after acceleration will also be able to ionise. This process continues and results in the formation of an avalanche, which rapidly builds up. Electrons move towards the 'head' of the avalanche, whilst ions move in the opposite direction (b).

When the number of electrons in the head approaches  $10^6$ , the avalanche begins to slow down due to the attraction of the positive ions. When  $10^8$  electrons are present in the head an electric field within the avalanche is created, which is in the opposite

sense to the electric field between the plates (c). Recombination of electrons and ions results within the avalanche and photons are emitted isotropically from the avalanche. The emitted photons cause ionisation of surrounding molecules in the vicinity of the original avalanche. The field in front and behind the original avalanche is enhanced, whilst the fields around the sides are suppressed. Thus ahead and behind of the original avalanche, new avalanches rapidly form (d) until the old and new avalanches merge, forming a streamer (e). The extremities of the streamer grow until they arrive at the plates. Thus the two plates of each module are connected by a low resistance conducting plasma of electrons and positive ions, which extends in a parallel direction to the electric field lines. A spark subsequently passes between the two plates.

## 2.4.2 Scintillators

Brigitte Burt

A scintillator is a material which converts some of the energy deposited by charged particles to visible light. The charged particle is generally set in motion by an interaction with x ray or gamma ray photons. The atoms of the material are readily excited by radiation. Light is released almost instantaneously as electrons return to the lower energy state.

Scintillators can be split into organic and inorganic substances. Sodium iodide, an inorganic scintillator, is normally of interest for the majority of photon energies used. There is interest in Bismuth Germanate (BGO) for the detection of high energy photons. Principles involved are in fact common to all scintillator types.

### Scintillator properties

The main properties are:

- Its ability to absorb energy from the incident radiation which is related to its atomic number and density.
- The fraction of absorbed energy which is converted into light photons.
- The spectrum of wavelengths of visible photons which it emits.
- The shape of the light output produced.

Material	Wavelength of Max Emission(nm)	Decay const	Refractive Index	Relative Density	Scintillation efficiency rel. to NaI(Tl)
NaI(Tl)	410	0.23	1.85	3.67	100
CsI(Na)	420	0.63	1.84	4.51	85
Bi <sub>4</sub> Ge <sub>3</sub> O <sub>12</sub>	480	0.3	2.15	7.17	8
CsF	395	0.075	1.55	2.5	10

Fig.19: Properties of some common scintillators

### Thallium-activated sodium iodide scintillator

Electrons in a pure crystal of sodium iodide are either in the conduction or valence band. Energy absorbed from charged particles allows electrons to be promoted from the valence to the conduction band where they are free to migrate through the crystal.

Subsequent electron-hole recombination results in the emission of energy once excited atom returns to ground state. The energy of photons produced in this manner does not fall in the visible region since the energy is too high. This results in the introduction of a small quantity of thallium impurity (about 1:1000 moles) which initiates an additional set of energy levels within the normally forbidden energy region between the valence and conduction bands. Electrons trapped at these sites emit visible light photons when they decay back to the valence band. These photons produced in the visible range can be attributed to the performance of the crystal as a scintillator.

NaI is about 10-15% efficient at converting charged particle energy into light photons. Once the light photons have been produced it is important for them to pass through the crystal to the photomultiplier tube which is only attached to one surface of the crystal. The crystal needs to be transparent to its own light photons and this is ensured by the fact that the photon energy is less than the main band gap of the crystal which is produced from the forbidden zone and so excitation of electrons from valence to conduction band does not occur.

Due to the hygroscopic nature of NaI it is kept in an air tight can usually made of aluminium except on the side where the photomultiplier is attached. This is made of either quartz or glass in order to keep the PMT protected from moisture. Exposure to moisture causes the sodium iodide crystal to turn yellow due to the release of free iodine through the absorption of much of the radiation induced fluorescence so that less light is emitted. Consequently this has the effect of reducing the signal available for detection of radiation.

At the surface to which the photomultiplier is attached the light photons have to travel from the crystal, through the window, through any intervening material and into the photomultiplier tube for processing. At each surface there is a mismatch of optical impedance and reflections arise, reducing the number of visible photons entering the photocathode. The interface can be removed through the introduction of silicon grease between photomultiplier tube and window of the scintillation detector.

### **Solid Organic Scintillators**

The main disadvantage with these scintillators stems from their low atomic number and density which diminish the efficiency with which they absorb energy from incident gamma photons. They are also relatively inefficient at producing light from the absorbed energy. These aspects result in organic -based scintillators having poor energy resolution.

Advantages of solid organic scintillators include their low cost, making large detectors affordable. The material is easily machined into required shapes and sizes since organic molecules can form polymers of various lengths. The hygroscopic nature associated with inorganic scintillators is not a factor so there is no need for the 'aluminium can'. This means that beta radiation and low energy x-ray and gamma photons can be measured.

## Light Guide

When the crystal window and photomultiplier tube are the same size they are coupled directly together with silicon grease between them. In other cases either when their sizes differ or there is a wish to transmit and distribute the light over a larger area of the tube, a light guide is used. The light guide is generally made of Perspex or similar material and is smoothly shaped to join crystal and tube surfaces, which are coated with reflective covering to reduce light loss. The light guide has the effect of increasing counting efficiency and positioning accuracy.

### 2.4.3 Cherenkov Radiation

CarolineRobson

This technique is used primarily for the detection of high energy cosmic  $\gamma$ -rays, which when incident upon the upper atmosphere lead to the production of electron-positron pairs. In 1934, while working under the supervision of S. I. Vavilov, Pavel Alekseyevich Cherenkov observed blue light emissions from water irradiated with radioactive particles. It was discovered that the particles were travelling at velocities faster than the speed that light could travel in the water.

When a particle passes through matter it polarizes then depolarizes the surrounding atoms. This causes an electromagnetic wave to spread out from the path of the particle. While the particle travels slower than the speed of light the wavefronts never meet and so do not interfere. If the particle is travelling faster than the speed of light and hence faster than the velocity of the emitted wavefronts, they overlap and interference occurs. This interference leads to an observable light pulse. The radiation can propagate in only one direction relative to the particle's velocity because only at one angle  $\theta$  will the wavefronts add up coherently according to Huygens' construction (see fig. 20, below).

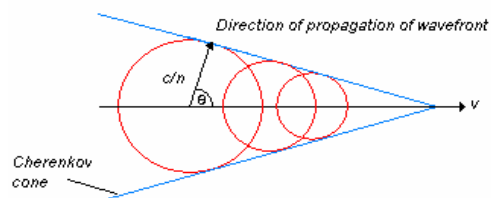


**Fig.20: Huygens construction for determining the direction of Cherenkov radiation wavefronts, where  $v$  is the velocity of the particle travelling through the medium**

An analogy to this situation is the 'sonic boom' produced by an aircraft as it exceeds the speed of sound. If the aircraft approaches at a speed very close to that of sound in air, it cannot be heard until it is almost overhead as it is almost keeping up with its sound. If it then accelerates to a speed greater than that of sound the waves come together behind the aircraft, creating a large pressure wave which we hear as a dull boom.

In the Cherenkov case the angle of propagation of the wavefronts i.e. the direction of the wavevector,  $\theta$ , is calculated by:

$$\cos \theta = \frac{c}{nv} \quad [3]$$

where  $v$  is the velocity of the particle,  $n$  is the refractive index of the medium and  $c/n$  is the velocity of light in the medium, which in the sparse gases of the upper atmosphere is almost equal to  $c$ . The Cherenkov condition states that the particle must be travelling faster than the speed of light in the medium, i.e. that:

$$v > \frac{c}{n} \quad [4]$$

If a  $\gamma$ -ray incident on the top of the atmosphere imparts enough energy to the electrons and positrons it creates, these particles can gain speeds greater than the speed of light in the atmospheric gas. The refractive index of the gas is only slightly higher than unity so in order to produce Cherenkov radiation the particles must travel at speeds very close to that of light in a vacuum i.e. at relativistic speeds. Many of the relativistic electrons and positrons are absorbed in the atmosphere but the Cherenkov radiation propagates to sea level .

### Threshold Detectors

The simplest type of detector is a threshold detector, which works by setting a threshold energy for the particles coming through. A material is selected with a refractive index such that only particles which obey the Cherenkov condition i.e. have velocities greater than the speed of light in that material, will be detected. For example, particles passing through plexiglass, which has a refractive index of  $\sim 1.5$ , would only emit Cherenkov light and therefore be detected if they have a velocity greater than  $0.67c$ . If particles with extreme relativistic energies are to be detected, gas detectors are used. Threshold detectors are used mainly for determining the nature of a particle where its momentum and energy are approximately known This is particularly useful in space where it is difficult to measure the wave vector and so only the optical emission is studied. By using several detectors with different thresholds i.e. a selection of gases at different pressures,  $v$  can be calculated without knowledge of the Cherenkov angle.

Differential Cherenkov detectors are slightly more advanced in that they can detect a range of velocities. They are usually set up with mirrors so that only a certain range of Cherenkov angles and hence velocities are detected.

Ring-imaging Cherenkov detectors make use of a spherical mirror to focus the Cherenkov light cone into a ring on an array of light detectors or a single detector that can determine the position of the incident light. The centre of the ring shows the path of the particle and the radius of the ring leads to the Cherenkov angle and the particle's velocity. This is achieved by reflecting the light from the inside of a spherical mirror whose focal length and rotation angle are known (See fig.21, overleaf). The direction of the particle can be determined using a silicon telescope, which consists of planes of pixels that register hits coming from different directions.

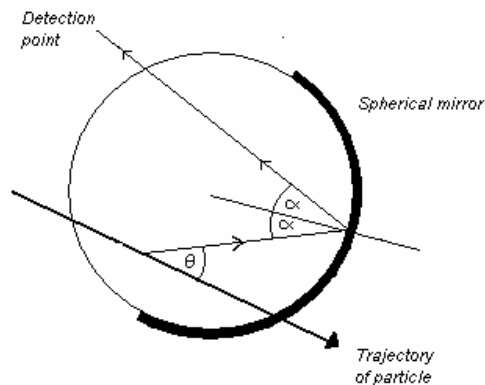


**Fig.21:** Schematic diagram of Cherenkov angle reconstruction using a spherical mirror

## Cherenkov Telescopes

Ground-based air Cherenkov telescopes (ACTs) are situated in several locations worldwide and are used to measure the light emissions from high-energy particles in the upper atmosphere. During extensive air showers, light is emitted within a cone of angle  $1-2^\circ$ . This is due to the angle of the Cherenkov cone being roughly this size but is also caused by the Coulomb scattering of electrons and positrons in the atmosphere, which results in them emitting along slightly different axes. The result of this is that the Cherenkov radiation is not focused on a single point but is instead spread over an area with a typical radius of 100m from the axis of the shower.

ACTs usually consist of an array of large mirrors, which focus the Cherenkov light from the air shower onto a corresponding array of photomultiplier tubes (PMTs) to form an image of the shower (See fig 22)

Properties of the image can be used to distinguish between  $\gamma$ -ray showers and those that have been created by hadronic cosmic ray particles. One of the main technical issues with ACTs is the elimination of background as the night sky background is about  $7 \times 10^{11}$  photons  $\text{m}^{-2}\text{s}^{-1}\text{sr}^{-1}$  but a typical Cherenkov incidence is only around 7 photons  $\text{m}^{-2}\text{s}^{-1}\text{sr}^{-1}$ . However, these arrive in bursts which only last in the region of 10ns so the background can be eliminated to an efficiency of 99.7% by accurate timing of the arrival of the light pulses detected by different elements of the array and the use of fast imaging cameras.



**Fig.22: The CANGAROO-II (Collaboration of Australia and Nippon for a GAMMA Ray Observatory in the Outback)** is a project based near Woomera in South Australia, which was set up to study sources in the southern sky that emit  $\gamma$ -rays in the TeV range. The 10m reflecting ACT is shown during the day in its stowed position ([www.icrhp9.icrr.u-tokyo.ac.jp](http://www.icrhp9.icrr.u-tokyo.ac.jp))

As the Cherenkov light comes from particles that don't usually reach ground level, ACTs can be used to detect  $\gamma$ -rays of very low energy but they can only operate on clear nights with no moonlight. Showers caused by cosmic ray nuclei can be distinguished from  $\gamma$ -rays because light from nuclear showers tends to be more random and diffuse. Showers produced by  $\gamma$ -rays are spread over a smaller area and are predominantly from point sources in a specific direction.

### Water Cherenkov Detectors

The refractive index of water is bigger than that of air such that light travels approximately 25% slower than in a vacuum. It is calculated that the number of photons per unit track length of charged particles passing through at a speed greater than that of light in the medium is greater than air by a factor of approximately 1400. The Cherenkov angle in water is also found to be much greater at  $41^\circ$  compared to a value of  $1^\circ$  in air. This results in a much wider and more intense cone of light.

The Milagro detector, built in January 1998 near Los Alamos, USA, consists of a large array of PMTs submerged in an 8 metre deep pond. One layer of PMTs is laid along the bottom of the detector (see fig.23, below) in order to detect the light produced by cosmic ray muons, which pass through the water without interacting, and another layer is closer to the surface to detect light produced by fast-moving electrons and positrons resulting from interactions with high-energy  $\gamma$ -rays that make it to the Earth's surface. The pond has a large field of view as it can detect particles travelling in directions close to horizontal.

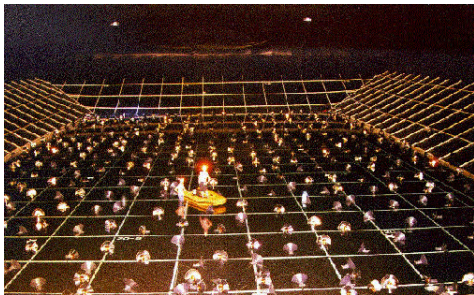


**Fig. 23: The Milagro detector during the filling process. Engineers carry out maintenance from an inflatable boat. ([www.icrhp9.icrr.u-tokyo.ac.jp](http://www.icrhp9.icrr.u-tokyo.ac.jp))**

Due to its large area the detector is sensitive to particles with energies as low as 4GeV (such as those emitted by the sun in coronal mass ejections) and hence is currently the world's most sensitive detector. As the Cherenkov angle is so much greater in water, the PMTs can be placed relatively much further apart than the mirrors of an ACT and still detect almost all high-energy particles that enter the pond. If the spacing is less than double the depth of the water above there are no 'gaps' where particles can go undetected.

Other well known water Cherenkov detectors include the Homestake Mine experiment in the USA and Super Kamiokande detector in Japan, which consists of a large cylindrical tank of water with PMTs on the inside wall. These are used for the detection of neutrinos.

## 2.5 Selection of a Detection Method

### Specification

The detector must be:

- Portable (carried by one or two people)
- Durable (able to withstand transportation in a vehicle or by foot and also must be able to cope with small impacts e.g. being knocked or kicked by accident)
- Cost-effective (we have to be able to afford to build it)
- Aesthetically pleasing (must look interesting)
- Demonstrable (we must be able to show how it works i.e. components visible)
- Safe (doesn't run the risk of injuring anyone)

After considering the various methods it was decided that a scintillation counter would be the most appropriate for a small, portable detector.

The spark chamber was discarded because the gas system would be too complicated to build in the time available and would also be very heavy but delicate, making it difficult to transport and unsuitable for school-based demonstrations. The high voltages and large discharges would also make it unsafe for school students to use.

A Cherenkov detector would also have been outside the scope of this project as it would require a large array of PMTs and either many reflecting mirrors or a large tank of a liquid such as water. Again portability and durability would be a problem as well as the cost of all the components. The elimination of background would be a particular problem and as the detector would have to be operated in darkness it would be unsuitable for a demonstration model. Cost would be a major issue.

A scintillation counter, although not without complicated technical issues, could be built to the above specification. Above all, it could be constructed as to be portable, durable and cost-effective.

## 2.6 Photomultiplier Tubes

An important component of any scintillation apparatus is a photomultiplier tube or array of photomultiplier tubes (PMTs). The primary function of a PMT is to convert an incoming optical signal, often very weak, to a stronger electrical signal which can then be handled more easily. Often used in conjunction with scintillating materials, these devices are employed in a wide variety of fields, for example medical imaging, radiation monitoring, X-ray diffraction, industrial material thickness gauging and the carbon-14 dating of archaeological artifacts as well as high energy particle physics applications such as detecting the trajectories of particles produced in accelerators.

A typical PMT consists of a photocathode, focusing electrodes, an electron multiplier made up of a number of dynodes and an anode, all encased inside a vacuum tube (see fig.24, overleaf). When a photon strikes the photocathode it causes an electron to be released, which is then focused onto the electron multiplier by the attractive or repulsive electrode voltages, depending upon the construction. Once amplified, the secondary electrons are attracted towards the anode to form the output signal.

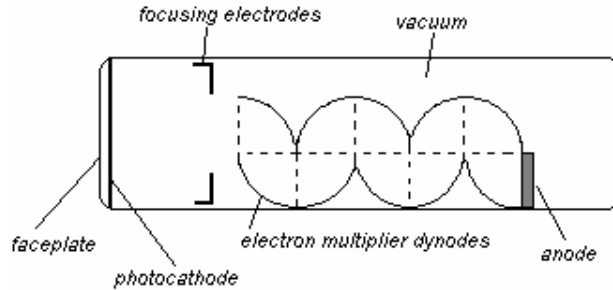


**Fig.24: Components of a typical photomultiplier tube**

Electron multipliers amplify the initial electron into a cascade by a process of secondary emission. This is achieved by a series of dynodes which, set to different voltages by a potential divider, typically release four electrons for each one absorbed. Thus for a multiplier containing  $N$  dynodes the amplification is  $4^N$ . Typical constructions for electron multipliers include the circular cage type, which is usually used in side-on PMTs and involves a circular array of dynodes and the box-and-grid type, used in head-on PMTs (see fig.24, above).

## 2.7 Optical Fibres

Rebecca Wong

### Wavelength Shifting (WLS) and clear fibres

An optical fibre consists of a single flexible rod of high refractive index with polished surfaces coated with transparent material of a lower refractive index. The coating, known as cladding, prevents light from leaking between fibres in close proximity. Light falling on one end within a certain solid angle will undergo total internal reflection at the surface of the core. The light is trapped within the core and travels in zigzag paths down the length of the fibre with little or no absorption. The fibre can continue to reflect light when it is considerably curved, as long as the reflection angle remains greater than the critical angle.

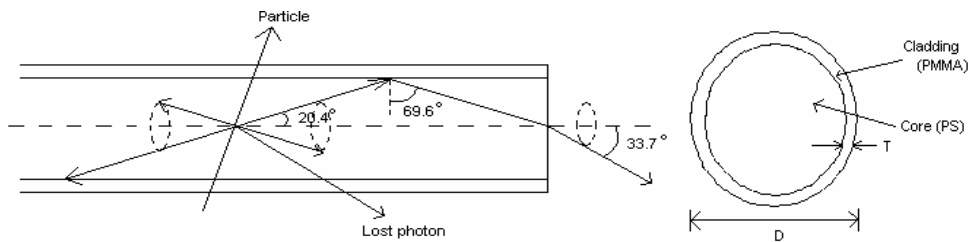
The WLS and clear fibres are a key part of the optical readout system of any scintillation apparatus. Each WLS fibre collects scintillation light from scintillator tiles and transmits it to a clear fibre, which is connected to the WLS by an optical connector, then to a PMT.

The scintillating core contains a combination of fluorescent dopants selected to produce the desired scintillation and optical resistance characteristics. For scintillation light transmission through WLS it is accomplished by the fluor which absorbs the blue light from the scintillator and re-emits it at a longer wavelength. Fig. 25, overleaf, shows the common properties of plastic fibres.

	Core	Cladding	
		for single cladding or inner for multi cladding	outer for multi cladding
<b>Material</b>	Polystyrene (PS)	Polymethyl methacrylate (PMMA)	Fluorinated PMMA (FP)
<b>Refractive index</b>	n = 1.59	n = 1.49	n = 1.42
<b>Density (g/cm<sup>3</sup>)</b>	1.05	1.19	1.43
<b>No. of atom per cm<sup>3</sup></b>	C : 4.9 x 10 H : 4.9 x 11	C : 3.6 x 10 H : 5.7 x 11 O : 1.4 x 10	

**Fig 25: Common properties of Plastic Fibres**

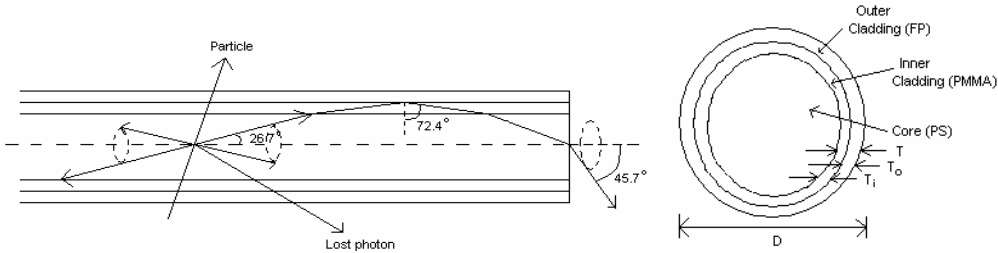
Multi-cladding fibre has higher light yield than single-cladding fibre because of its larger trapping efficiency (see figs 26 and 27, below).



**Single cladding:**

Cladding thickness (T) = 3% of D; Numerical Aperture (NA) = 0.55; Trapping efficiency = 3.1%

**Fig.26: Typical transmission mechanism, cross section and cladding thickness of a round multi-cladding fibre**



**Multi-cladding:**

Cladding thickness (T) = 3% (T<sub>o</sub>) + 3% (T<sub>i</sub>) = 6% of D  
Numerical Aperture (NA) = 0.72; Trapping efficiency = 5.4%

**Fig.27: Typical transmission mechanism, cross section and Cladding thickness of a round multi-cladding fibre**

The refractive indices of the core and cladding and the cross section of the fibre determine the trapping efficiency. In round fibres, the trapping efficiency also depends on the distance between the fibre axis and the scintillation event. The trapping efficiency is:

$$e = 1/2 \cdot (1 - n_2^2/n_1^2) \tag{5}$$

Where  $n_1$  = refractive index of the core and  $n_2$  = refractive index of the cladding

The numerical aperture (NA) stated in figs 26 and 27 is a measurement of the ability of an optical fibre to capture light. The aperture is the conical aperture through which light must pass to be captured in the core, i.e.

$$NA = n_o \cdot \sin (a_o) = (n_1^2 - n_2^2)^{1/2} \quad (6)$$

where  $n_o$  = refractive index of the surrounding medium,  $n_1$  = refractive index of the core,  $n_2$  = refractive index of the cladding,  $a_o$  = critical angle to the optical axis.

Very little light intensity is lost in the fibres as a result of reflections on the sides. Any reduction in intensity is due essentially to reflections from the two ends and absorption by the fibre materials.

The light yield calculation can be factorised in three parts:

- The transport of scintillation photons of an absorption point in a WLS fibre.
- The transport of re-emitted (wavelength-shifted) photons through the WLS fibre, connector and clear fibre.
- The photoelectron emission and amplification within the PMT.

To get a maximum light yield, the WLS fibres have to have the following requirements:

- The absorption spectrum of the fibre should match the emission spectrum of the scintillator and the emission spectrum of the fibre should match the quantum efficiency of the photomultiplier.
- The fibres should have a maximum light yield and attenuation length. The upper limit of the light yield is given by the refractive indices of the materials.
- The fibres should be flexible and suffer minimum damage caused by stress due to the curvature on the paths in the scintillator.